Deactivation phenomena during catalytic wet air oxidation (CWAO) of phenol over platinum catalysts supported on ceria and ceria–zirconia mixed oxides

S. Nousir [a], S. Keav [b], J. Barbier Jr. [b,*], M. Bensitel [a], R. Brahmi [a], D. Duprez [b]

[a] University of Chouaib Doukkali, Laboratoire de Catalyse et Corrosion des Matériaux, Department of Chemistry, Faculty of Sciences of El Jadida, BP. 20, 24000 El Jadida, Morocco
[b] University of Poitiers, LACCO UMR CNRS 6503, Laboratoire de Catalyse par les Métaux, 40 Avenue du Recteur Pineau, F-86022 Poitiers Cedex, France

ABSTRACT

Catalytic wet air oxidation (CWAO) of aqueous solution of phenol was carried out with pure oxygen at 160 °C in a stirred batch reactor on platinum supported oxide catalysts (Pt/CeO_2 [c] calcined at 650 and 800 °C and $Pt/Ce_xZr_{1-x}O_2$ with $x = 0.90, 0.75$ and 0.50). The catalysts were characterized before (BET, FT-IR spectroscopy, hydrogen chemisorptions, oxygen storage capacity (OSC)) and after reaction (TPO, elementary analysis, GC–MS and DTA–TGA). The results demonstrate a poisoning of the catalysts during CWAO reaction due to the formation of different forms of carbon deposit on the materials: carbonates and polymeric carbon species. This poisoning phenomenon is limited by the introduction of 50% of zirconium into ceria lattice for the catalysts presenting the lowest surface area. Polymeric deposits play a major role in the catalyst deactivation.

© 2008 Elsevier B.V. All rights reserved.

1. Introduction

The wet air oxidation (WAO), first patented over 50 years ago [1], uses oxygen or air to fully oxidize organic compounds to carbon dioxide and water [2]. It is a clean process not involving any harmful chemical reagent. However, being a non-catalytic process, it requires high temperature and high pressure of oxidant to achieve a complete oxidation in a reasonable reaction time. This induces high operating costs, which limits the development of WAO processes. The use of catalysts (CWAO) greatly improves the degradation of organic pollutants by using a lesser amount of oxidizing agent and milder conditions of temperature and pressure [3]. The use of solid catalyst offers a further advantage compared with homogeneous catalysis, in principle the catalyst being easily recovered, regenerated and reused. Heterogeneous catalysts containing platinum appear like a very good alternative for this process; in addition to their high activity, their stability in reaction is a principal asset. Indeed, these materials are able to totally

transform the most refractory molecules like acetic acid [4] and phenol. Due to the low solubility of oxygen under the reaction conditions, the limiting stage of the process is the transfer of O_2 from the gas phase to the active catalytic site. This is why the development of catalysts supported on oxides like ceria was undertaken. These materials, known for their redox properties, particularly in the field of automobile depollution [5], are able to store oxygen reversibly. Nevertheless, it is possible to improve the catalytic properties (i) by modifying on the metal/support interface and (ii) by introducing into the structure of ceria doping agents presenting the required characteristics to amplify both oxygen transfer phenomena and catalyst stability. The role of metal/support interactions and oxygen transfer on the catalytic activity justify that this study was devoted to the influence of the specific surface area and of Zr content on the catalytic performances of $PtCeO_2$. Phenol was chosen as a reference molecule for the following reasons: (i) it is refractory to the biological process [6], (ii) it is involved as intermediary compound in the oxidation scheme of many aromatic molecules [7]. Its presence in water, at very low concentrations (ppb order), is enough to insufflate unpleasant odor and taste [8]. Phenol is extremely toxic for human being and resists to biological treatments [9]. The acceptable

---

maximum concentration (MATC for maximum acceptable toxicant concentration) is fixed at 77 $\mu g\,L^{-1}$ of phenol [10]. Devlin and Harris have studied the non-catalyzed phenol oxidation in aqueous solution by molecular oxygen [11]. On the basis of the various intermediates detected during the reaction, they proposed a reaction pathway, also validated in the presence of catalysts. During the CWAO reaction, phenol is partially transformed into carboxylic acids like acetic acid, which is produced at the final stage of the reaction and represents one of the most refractory by-products [12,13].

In addition of leaching, the second major cause of catalyst deactivation in CWAO is the formation of carbon-adsorbed compounds limiting the access of reagents to the active sites. This phenomenon concerns both metallic oxides [14,15] and supported noble metals [14–18]. Hamoudi et al. measured, respectively, 43% and 50% of carbon covering the surface of Pt/Al_2O_3 and Mn/Ce catalysts after reaction [14]. The carbon adsorbed compounds are formed by (i) by-products of phenol decomposition strongly adsorbed on the catalyst surface and (ii) compounds with high molecular weight resulting from the polymerization of glyoxal and its condensation products with phenol [19,20]. The formation of this "coke" is favored at reaction temperatures lower than 150 °C and for important phenol concentrations [9,14]. The catalyst can recover its initial activity after regeneration at 400 °C under air [18] or after a rinsing by acetone [16]. Mikulová et al. [4] has shown that the presence of carbonate species in the lattice of the support, formed during the reaction, is also responsible to a deactivation phenomenon linked to an inhibition of oxygen transfer.

The objective of this paper is to study in detail the nature of this carbon-containing deposit (CCD) (carbonate species and carbon-adsorbed compounds) leading to the deactivation of Pt/CeZrO$_x$ catalysts in CWAO of phenol.

2. Experimental

2.1. Preparation

In this study, the $Ce_xZr_{1-x}O_2$ supports (with x = 0.90, 0.75 and 0.50) were synthesized via a precipitation method. Appropriate amounts of nitrate salts (cerium nitrate: $Ce(NO_3)_3 \cdot 6H_2O$ (2.33–4.2 g) and zirconyl nitrate: $ZrO(NO_3)_2 \cdot 2H_2O$ (0.41–2.07 g)) were dissolved in 40 mL of distilled water in order to have the specified Ce/Zr ratios. Aqueous ammonia (12 mL, 28%) solution was added drop wise until pH reached a value of 9 then the stirring was stopped. The precipitate thus obtained was filtered and washed with dilute ammonia solution (0.25 mol L^{-1}) and distilled water, and then dried at 120 °C overnight. All three supports were calcined under static air for 6 h at 450 °C. CeO_2 is a commercial rare earth ceria HSA 5 provided by Rhodia rare earths and it was chosen to compare with the new supports calcined at 650 and 800 °C.

The 2.5 wt.% Pt/$Ce_xZr_{1-x}O_2$ (x = 1, 0.90, 0.75 and 0.50) catalysts were prepared in a rotating evaporator by impregnation and dry evaporation using aqueous solution of $Pt(NH_3)_6(OH)_2$ as a metallic precursor salt. This solution was completed by distilled water up to 8 mL solution per gram of support. The catalysts were dried overnight at 120 °C, calcined under O_2 at 400 °C for 4 h and finally, activated by reduction under H_2 (30 mL min^{-1}) for 3 h at 350 °C to obtain platinum in the metallic state.

2.2. Characterizations of fresh and used catalysts

2.2.1. BET surface area

The specific surface areas of the collected powders were measured by nitrogen adsorption at 77 K using the BET method (Micrometrics ASAP 2010). Prior to analysis, the samples were outgassed at 453 K for one night under high vacuum.

2.2.2. Dispersion

Hydrogen chemisorptions were used to determine the metal dispersion of catalyst. This characterization has been carried out in a chromatographic micro-reactor [21]. After a reduction under H_2 (350 °C, 1 h) and degassing under argon (350 °C, 3 h), hydrogen pulses (0.26 mL) were injected at regular interval of time at −85 °C [22] to avoid hydrogen spillover. Ultrapure H_2 and Ar (less than 1 ppm impurities) were used throughout this technique of characterization. The calculation of the particle sizes is performed with the cubic model corresponding to the Hughes hypothesis [23] (Eq. (1)):

$$d\,(nm) = 5 \times 10^5 \frac{M}{\rho DS} \frac{100.6}{D} \tag{1}$$

where 5 corresponds to the number of exposed faces, M is the molar weight of Pt (192 g mol^{-1}), ρ is the metal density (21.45 g mL^{-1}), D is the dispersion (%) and S is the surface of 1 mol of Pt [24] (45293 $m^2\,mol^{-1}$).

2.2.3. OSC

Oxygen storage capacity (OSC), described earlier [4,25], was measured at 200 and 400 °C under atmospheric pressure. The number of oxygen atoms layers (NL, Eq. (2)), involved in the storage process, is calculated on the basis of the theoretical number of reducible surface oxygen atoms (O_{surf}, Eq. (3)) and the OSC of metal (OSC_{met}, Eq. (4)), OSC_{met} = number of oxygen atoms necessary for the oxidation of accessible Pt atoms (PtO) [26] and OSC of the support is deduced from the OSC measured and OSC of metal (OSC_{sup}, Eq. (5)).

$$NL = \frac{OSC_{meas} - OSC_{met}}{O_{surf}} \tag{2}$$

$$O_{surf} = \frac{bS}{Na^2} \tag{3}$$

$$OSC_{met} = \frac{Dw_{Pt}}{M_{Pt} \times 10000} \tag{4}$$

$$OSC_{sup} = OSC_{meas} - OSC_{Pt} \tag{5}$$

S = BET surface area ($m^2\,g^{-1}$), a = lattice parameter (m), N = Avogadro number, b = fraction of reducible elements (Ce) in the unit cell (1, 0.90, 0.75 and 0.50), w_{Pt} = weight percent of Pt and M_{Pt} = molar weight of Pt. In these equations, it is supposed that surface platinum only can be oxidized or reduced, the bulk of Pt particles remaining in the Pt^0 state throughout the OSC measurement.

2.2.4. C–O–H elementary analysis

Carbon, oxygen and hydrogen in the CCD are quantified on an elementary analyzer (C.E. Instruments NA2100 PROTEIN). It consists in performing a complete combustion of the sample at 950 °C catalyzed by tungsten and copper oxides. The gases produced were separated on an activated carbon column and quantified using a catharometer. The analysis of the results was carried out using the Eager 2000 software.

2.2.5. TPO

TPO measurements were used to characterize the CCD present on the catalyst surface after CWAO. A known quantity of solid (5 mg) was placed in a quartz reactor then heated at 7 °C min^{-1} up to 700 °C under a flow of 1%O_2/He (12 mL min^{-1}). The water

produced during the reaction was trapped by a desiccant. Carbon dioxide and oxygen in the dried gas were analyzed every minute by catharometry.

2.2.6. DTA–TGA analysis

Differential thermal and thermogravimetric analyses (DTA–TGA) were carried out in a MT Instruments SDT Q600 apparatus under an air flow of 100 mL min^{-1}. After stabilization at 25 °C, the temperature was increased at 2 °C min^{-1} up to 650 °C. The thermograms were processed using the Universal Analysis software.

2.2.7. GC–MS analysis

A 400 mg weight of used catalyst was treated in a soxhlet with methylene chloride, according to the procedure previously described by Guisnet and Magnoux [27]. The catalyst was exposed to the reflux of the condensing solvent for 6 h. The extract was afterwards evaporated in a rotating evaporator and analyzed by gas chromatography coupled with mass spectroscopy. The Varian CP3800 gas chromatograph was equipped with a Macherey-Nagel column (30 m × 0.25 μm × 0.25 mm). A 1 μL volume of sample was injected for each analysis, the split ratio being set at 15/1 and the flow rate of Helium at 1.0 mL min^{-1}. Mass spectra were recorded in the mass range from 50 to 500 amu on a Varian 1200 TQ mass spectrometer operating in electronic impact mode. The column temperature program was in the range 50–300 °C.

2.3. Catalytic test

Catalytic wet air oxidation (CWAO) reactions were carried out in a 0.44 L Hastelloy C22 autoclave as described elsewhere [28]. The stirring rate of the turbine was 400 rpm. To optimize the oxygen dissolution and to permit a good contact between the reactants and the catalytic powder dispersed in solution, the stirring rate of the turbine was 400 rpm. This stirring rate was chosen from the range of stirring rates corresponding to the kinetically limited regime to avoid (i) the mass transfer limited regime as well as (ii) too violent stirring causing mechanical damage of catalyst and of reactor.

The reaction temperature was 160 °C. 160 mL of aqueous solution, containing phenol ([phenol] = 22.3 mmol L^{-1}) and 4 g L^{-1} of catalyst powder, were introduced into the reactor. The reaction starts after addition of 2 MPa oxygen pressure. At appropriated intervals of time, gas and liquid aliquots were sampled and analyzed by GC and HPLC in order to follow the effluent composition [25]. Mineralization molar ratio, activity and turn over frequency were calculated. The mineralization molar ratio (%M) (Eq. (6)) corresponds to the ratio of the CO_2 formed, expressed in mol C L^{-1} ([CO_2]$_t$), and the initial total organic carbon (in mol C L^{-1}). The [CO_2]$_t$ corresponds to the total CO_2 present both in the gas and in the liquid phase ([CO_2]$_t$ = [CO_2]$_{gas}$ + [CO_2]$_{liq}$). The CO_2 of the liquid phase is obtained from specific studies concerning the CO_2 equilibrium between the two phases under 2 MPa at different temperatures [29]. The catalytic activity (A) is the amount of CO_2 formed in 1 h of reaction per gram of metal and per hour (mmol CO_2 g^{-1} h^{-1}) (Eq. (7)). Turn over frequencies (h^{-1}) were calculated (Eq. (8)) with the value of mineralization (1 h, %) and allowed to compare the catalyst behavior in our specific experimental conditions.

$$\%M = 100 \times \frac{[CO_2]_t}{TOC_i} \tag{6}$$

$$A = \frac{6M_{1h}[PhOH]_i}{m_{cata}w_{Pt}} \tag{7}$$

$$TOF = \frac{AM_{Pt}}{10D} \tag{8}$$

where [PhOh]$_i$ is the initial concentration of phenol in mmol L^{-1}, six is the number of C atoms in C$_6$H$_5$OH, w_{Pt} is the wt.% of platine, m_{cata} is the mass of catalyst (g L^{-1}), M_{Pt} is the molar weight of Pt (g Mol^{-1}) and D is the dispersion (%).

The conversion of phenol (%C) was also calculated (Eq. (9)):

$$\%Conv = \frac{[PhOH]_i - [PhOH]_t}{[PhOH]_i} \times 100 \tag{9}$$

$$S\,(\%)\;CO_{2\,3h}100 \times \frac{\%M_{3h}}{\%Conv} \tag{10}$$

where [PhOH]$_i$ and [PhOH]$_t$ are, respectively, the initial and the instantaneous concentration of phenol (mol L^{-1}). $S\,(\%)\;CO_{2\,3h}$ (Eq. (10)) corresponds to the selectivity in CO_2 at 3 h (%).

The total organic carbon, which corresponds to the total amount of dissolved carbon in water (filtered samples), was measured with an O. I. Analytical, Model 1020A TOC analyzer which employs high temperature combustion oxidation, coupled with a no dispersive infrared detection technology. TOC abatement is determined by (Eq. (11))

$$\%\Delta TOC = \frac{TOC_i - TOC_t}{TOC_i} \times 100 \tag{11}$$

TOC_i and TOC_t correspond, respectively, to the TOC values of the initial solution and the analyzed samples.

3. Results and discussion

3.1. Fresh catalyst characterizations

3.1.1. BET and particle size measurements

Specific surface area values of the materials as well as metal dispersions and crystallite sizes of Pt given by H$_2$ chemisorptions, are presented in Table 1. The thermal treatments at 650 and 800 °C lead to a decrease in specific surface areas of the commercial ceria respectively from 190 to 97 m^2 g^{-1} and 190 to 45 m^2 g^{-1}. After metal addition, a decrease in BET values is observed for all the catalysts supported on CZ especially for PtCZ(50). The catalysts impregnated on CeO$_2$ or on mixed oxides Ce$_x$Zr$_{1-x}$O$_2$ present relatively high dispersions. The particle sizes increase slightly when the BET areas decrease. This can be explained by a strong interaction between the metal and the support. The method of impregnation performed in basic medium induces the exchange between cationic form of Pt[[Pt(NH$_3$)$_6$]$^{2+}$(OH)$_2$$^-$] and ceria, which favors high dispersions of platinum.

3.1.2. OSC measurements

OSC measurements are reported in Table 1 for the supports and the catalysts. Concerning the bare support the temperature of 200 °C is too low to activate the oxygen transfer process. OSC is not assessable in our reaction conditions at this temperature. At 400 °C and for a given material, the NL value is constant and rather low at 400 °C. The CZ OSC values are two times higher than those of Ce but remain always lower than 1. In the presence of metal, the results show that the OSC values of the PtCe catalysts decrease with the specific surface areas. However, in agreement with previous results, the addition of platinum significantly improves the migration of oxygen species in the support [26]. The NL values are then amplified by the presence of the metal but O_{surf} is always higher than OSC$_{sup}$ for the PtCe catalysts. On pure ceria, this process occurs only at the catalyst surface even in the presence of platinum. On the other hand, for the PtCZ catalysts, a positive effect

Table 1
Surface areas of the various samples and supports, dispersion and metallic crystallite sizes determined by H_2 chemisorption and oxygen storage capacity measurements

Samples	BET ($m^2 g^{-1}$)	D (%)	d_{Pt} Chim. (nm)	Oxygen storage capacity (μmol O g^{-1})				
				OSC_{meas}	OSC_{Me}	OSC_{sup}	O_{surf}	NL
Ce^c_{400} *	190	–	–	189	0	189	964	0.2
Ce^c650_{400}	97	–	–	95	0	95	492	0.2
Ce^c800_{200}	46			0	0	0	233	0
Ce^c800_{400}	46	–	–	45	0	45	233	0.2
$CZ(90)^{**}_{400}$	73	–	–	150	0	150	333	0.4
$CZ(75)_{400}$	98	–	–	163	0	163	372	0.4
$CZ(50)_{400}$	94	–	–	100	0	100	238	0.4
$PtCe^c_{400}$	184	63	1.6	820	81	739	933	0.8
$PtCe^c650_{400}$	96	55	1.8	327	71	256	487	0.5
$PtCe^c800_{200}$	45	41	2.5	68	53	15	228	0.1
$PtCe^c800_{400}$	45	41	2.5	161	53	108	228	0.5
$PtCZ(90)_{200}$	59	52	1.9	131	67	64	270	0.2
$PtCZ(90)_{400}$	59	52	1.9	559	67	492	270	1.8
$PtCZ(75)_{400}$	84	49	2.0	1188	63	1125	319	3.5
$PtCZ(50)_{400}$	50	39	2.6	1407	50	1357	126	10.8

* The subscript number corresponds to the OSC temperature condition.
** In parentheses (the proportion of ceria in the support lattice).

of zirconium insertion is clearly observed on OSC values. The presence of platinum permits to increase the oxygen transfer phenomena with the participation of several oxide layers. In this case, the oxygen atoms involved in the process come both from the surface and the bulk of the catalyst. The highest NL value is obtained for PtCZ(50) (1407 μmol O_2 g^{-1}). At equivalent BET surface area, its oxygen storage capacity is 20 times higher than those of PtCe^c800. It appears clearly that the introduction of zirconium into the lattice of ceria increases significantly the mobility of oxygen atoms.

Due to the low temperature of CWAO reaction the rate of oxygen transfer is lower than those obtained at 400 °C, but some OSC measurements performed at 200 °C reveal that the same benefit effects of noble metal and zirconium doping remain present at this low temperature. These results were previously obtained in the literature [26]. Even if the values are lower, the same material classification is observed.

3.2. Catalytic test results and characterizations after reaction

3.2.1. CWAO

CWAO of phenol was carried out at 160 °C on impregnated catalysts containing ceria and ceria–zirconia. Figs. 1 and 2(a and b), respectively, represent the evolutions of phenol mineralization (%M), phenol conversion (%Conv) and total organic carbon abatement (%ΔTOC) versus reaction time.

First of all, it is interesting to note that, during these experiments, the reaction medium becomes yellow colored. This phenomenon is similar to the formation of quinones [30], which gives color varying between orange yellow and brown according to their concentrations in solution. It could be seen that color intensifies and then weakens during the reaction, pointing out the accumulation and then the consumption of intermediary compounds. Moreover, the initial pH value of 4.6 of the reactant solution decreases rapidly and stabilizes near 2.3. This phenomenon confirms the formation of intermediary carboxylic acids resulting from the incomplete oxidation of phenol. On the bare support CZ(50), very low mineralization (15%) is obtained after 3 h of reaction (Fig. 1). Its promotion by platinum induces a reduction of its specific surface area from 94 to 50 m^2 g^{-1} but leads to a large increase of the mineralization ($M_{3 h}$ = 57%). On pure ceria, in term of mineralization at 3 h, the PtCe^c800 appears as the most active. It is able to convert, in 3 h, approximately 53% of initial phenol into CO_2. These results seem to indicate, surprisingly, that in the case of

catalysts supported on ceria, weaker are the values of specific surface areas, higher are the mineralization values after 3 h. This mineralization increases slightly by the introduction of 10% of zirconium, whereas the introduction of 25% of Zr is harmful. The mineralization values determined after 3 h permit to establish the following classification of catalysts: PtCZ(50) > PtCZ(90) > PtCe^c800 > PtCe^c650 > PtCe^c > PtCZ(75) > CZ(50) > blank.

Phenol conversion and the TOC abatement values for each catalysts versus reaction time are presented, respectively, on Fig. 2(a and b).

Without catalyst (blank experiment), 25% of the initial phenol is converted after 3 h of reaction. The %ΔTOC reached only a low value of 7% after 100 min of reaction even if the conversion (%Conv) increases steadily. For the bare CZ(50) support and compared to the experiment carried out without catalyst, the %Conv and %ΔTOC values increase by a factor of 1.5 and 4.8, respectively. The catalytic activity is greatly improved by platinum addition. Consequently, the use of catalyst activates considerably the phenol conversion
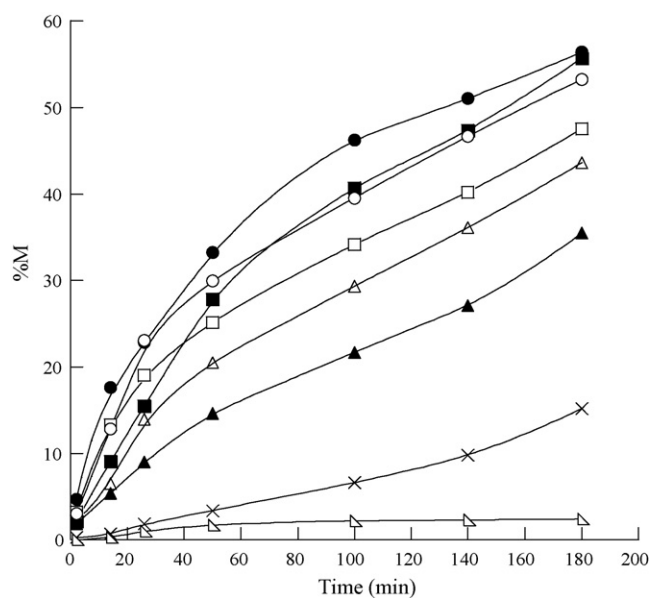

Fig. 1. Mineralization versus time for the various platinum catalysts impregnated on pure ceria: –○– PtCe^c800, (□) PtCe^c650, (△) PtCe^c, ceria–zirconia: (■) PtCZ(90), (▲) PtCZ (75), (●) PtCZ(50), the support (×) CZ(50) and (——△——) blank.

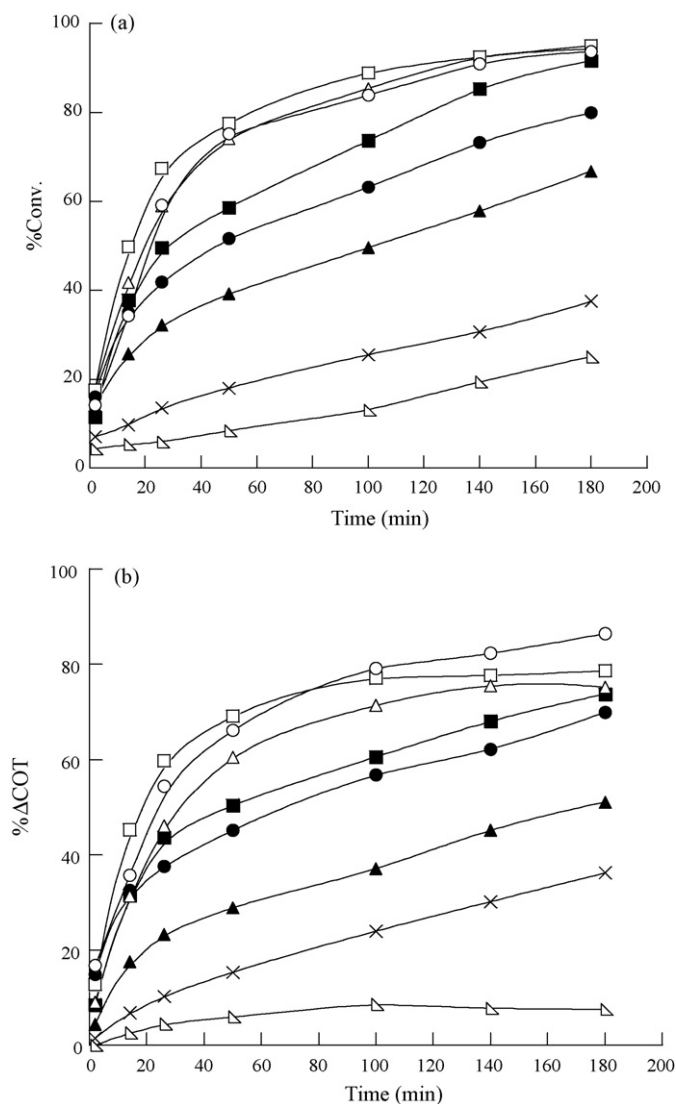**Fig. 2.** Conversion (a) and %ΔTOC (b) as a function of time for the various platinum catalysts impregnated on pure ceria: (○) PtCe^{c}800, (□) PtCe^{c}650, (△) PtCe^c, ceria–zirconia: (■) PtCZ(90), (▲) PtCZ (75), (●) PtCZ(50), the support (×) CZ(50) and (──△──) blank.

but also the degradation of the intermediary by-products. 94% of phenol conversion is obtained after 180 min of reaction by using a catalyst containing Pt supported on pure ceria (Fig. 2a). This conversion can be also reached for the CZ catalyst rich in cerium PtCZ(90). The Fig. 2b shows that the PtCe^{c}800 catalyst is the most powerful for the TOC abatement since 87% of %ΔTOC is obtained after 180 min of reaction. On the other hand, the comparison between the %Conv and the %M values indicates that the PtCe catalysts are less selective into CO_2 than those deposited on mixed oxides. Although, Ce promotes phenol conversion, it presents a lower ability for mineralization than CZ.

The difference between the values of %Conv and %ΔTOC, represented in Fig. 3, suggests that a significant part of phenol is converted into soluble organic by-products such as carboxylic acids, quinones and other intermediates [11]. Compared to the bare CZ(50) support, it appears clearly that the metal addition, by increasing phenol conversion, amplifies the proportion of by-products in the reactant medium and the CO_2 selectivity. The classification, in term of selectivity after 3 h of reaction (S(%) $CO_{2\ 3\ h}$,) is the following:

PtCZ(50) = 71% > PtCZ(90) = 61% > PtCe^{c}800 = 57% > PtC-
PtCZ(75) = 53% > PtCe^{c}650 = 50% > Pt-
PtCe^c = 46% > CZ(50) = 40% > > blank = 10%.

The lower the surface area, the higher selectivity into CO_2 after 3 h. This latter is amplified in the presence of Zr.

3.3. Study of the catalyst poisoning

3.3.1. Carbon-containing deposit

The differences between the values of %ΔTOC and %M give the fraction of the initial carbon in C_6H_5OH not analyzed as CO_2 or organic carbon at time t (Fig. 4). This figure confirms the presence of insoluble and/or CCD on the catalyst surfaces. On the bare support these species increase gradually versus reaction time. In the presence of platinum, these insoluble species strongly increase at the beginning of the reaction and then are stable on CZ catalysts or slowly decomposed on Ce catalysts. Nevertheless, the contents of insoluble carbonaceous species (adsorbed or not) are lesser on PtCZ catalysts than on PtCe ones. The classification of catalysts obtained after 3 h of reaction is: PtCZ(50) < PtCZ(75) < PtCZ(90) < CZ(50) < PtCe^{c}800 < PtCe^{c}650 ≈ PtCe^c. If noble metal catalysts are able to easily convert phenol, the intermediary
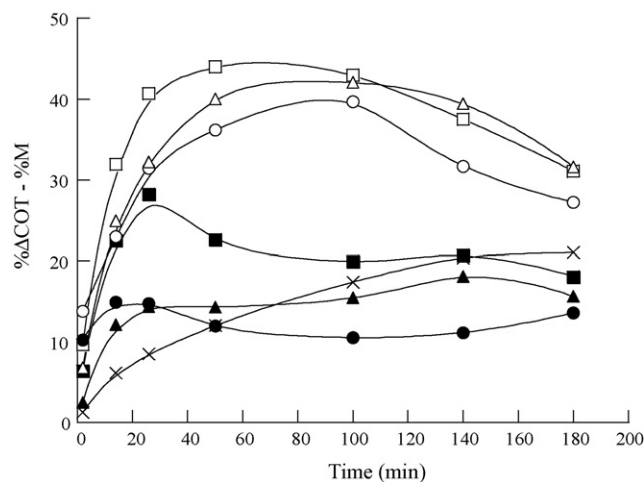

Fig. 3. Evolution of %Conv–%ΔTOC at 180 min for the various catalysts.

Fig. 4. Evolution of %ΔTOC–%M versus time for the various platinum catalysts impregnated on pure ceria: (○) PtCe^{c}800, (□) PtCe^{c}650, (△) PtCe^c, ceria–zirconia: (■)PtCZ(90), (▲) PtCZ (75) and (●) PtCZ(50) (×) CZ(50).
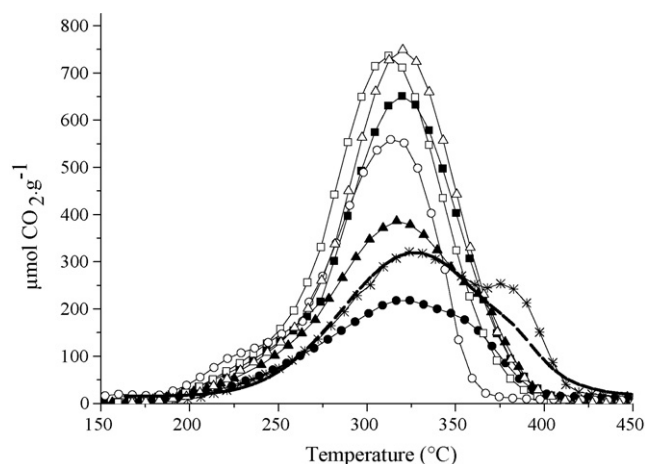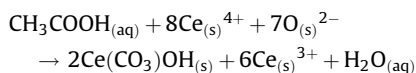
Fig. 5. TPO profiles of used catalysts. CO_2 formation: (○) PtCe^{c}800, (□) PtCe^{c}650, (△) PtCe^c, ceria–zirconia: (■)PtCZ(90), (▲) PtCZ(75) and (●) PtCZ(50) (×) CZ(50), O_2 consumption (– – –) CZ(50).

compounds resulting from its oxidation can be accumulate in the reactant medium.

The catalyst deactivation in CWAO results generally from the formation of CCD limiting the oxygen transfer and the access of the reagents to the active sites. This CCD consists of (i) by-products resulting from phenol polymerization (polymeric carbon species) [20], strongly adsorbed on the catalytic surface and, (ii) carbonate species, inserted in the lattice of the support and coming from the reduction of the Ce^{4+} ions by carboxylic acids (like acetic acid) present in the medium according to the following reaction: (Eq. (12)) [28].

$$CH_3COOH_{(aq)} + 8Ce_{(s)}^{4+} + 7O_{(s)}^{2-}$$
$$\rightarrow 2Ce(CO_3)OH_{(s)} + 6Ce_{(s)}^{3+} + H_2O_{(aq)}$$

In order to have more information on the nature of these adsorbed species and to determine if both carbonates and "polymeric carbon species" are present on the used catalysts, complementary analyses such as TPO, elementary analysis, DTA–TGA and GC–MS have been carried out on the catalysts after CWAO reaction.

3.3.2. Characterizations of used catalysts

Used catalysts were characterized first by Temperature Programmed Oxidation (TPO). The amounts of carbon dioxide formed versus the temperature are represented for each catalyst in Fig. 5. For the bare support (CZ(50)), the O_2 consumption is also presented. The bare support presents two peaks corresponding to the two types of poisons: the smallest one, at high temperature ($\sim$375 °C), with a low O_2 consumption, could be attributed to the

decomposition of carbonate species (Eq. (16)) and the largest one ($\sim$325 °C) to the polymeric carbon species (Eq. (17)). For this peak the O_2 consumption is rather equivalent than the CO_2 production. This point will be discussed afterwards. In the presence of platinum, only one CO_2 peak is observed when the CDD loading are high. In the case of PtCZ(50) and PtCZ(75), where CCD loading are lower, a shoulder, near to 360 °C, is, once again, observable. This indicates that in the presence of metal, all the CCD (if both present) would be oxidized or decomposed in a very weak range of temperature. As it was previously noted (Fig. 4), platinum promotes the CCD formation and the zirconium limits this deposit when the Zr contents are higher than 10%. Note that, whatever are the catalysts, the CCD is formed during the CWAO reaction. The highest values of NL obtained in the presence of platinum on CZ(50) support induces a limitation or an easier conversion of the CCD by amplifying the oxygen transfer phenomena.

Table 2 presents the results obtained by TPO, elementary analysis and DTA–TGA. n(C), n(O) and n(H) are, respectively, the molar contents (in mmol g^{-1}) of carbon (average value of TPO and EA), oxygen (from DTA–TGA) and hydrogen (from elementary analysis (EA)). The weight loss, measured by DTA–TGA, is determined in the 150–450 °C temperature range and corresponds only to the carbonaceous species removal.

n(C), n(H) and n(O) (in mmol g$^{-1}_{cata}$) are calculated, respectively, from the Eqs. (13–15).

$$n(C) = \frac{(\%C_{(TPO)} + \%C_{(EA)}) \times 1000}{2M(C) \times 100} \tag{13}$$

$$n(H) = \frac{\%H_{(EA)} \times 1000}{M(H) \times 100} \tag{14}$$

$$n(O) = \frac{\%O_{(DTA-TGA)} \times 1000}{M(O) \times 100}$$
$$= \frac{(\%Loss - \%C_{(EA)} - \%H_{(EA)}) \times 1000}{M(O) \times 100} \tag{15}$$

where M(C), M(H) and M(O) are the molar weights (g mol^{-1}).

The global ratios n(O)/n(C) are in the range 0.5–1.5 which indicates that oxygen contents of CCD are high. Moreover, in order to identify clearly the nature of CCD, polymeric carbon species were extracted by CH_2Cl_2 for 6 h at 40 °C and analyzed by GC–MS (Fig. 6). The nature of identified polymers adsorbed on the catalyst surface has a rather similar structure than those of phenol and coming from phenol polymerization. The formula of this "coke" is close to C_6H_6O with a n(O)/n(C) close to 1/6. As the global content of the deposit is largely higher, this means that carbonate species, (like (OH(CO$_3$))) in the lattice of the support are always present in the catalysts after the reaction.

Considering that the CCD is made up both of hydroxycarbonates ((OH(CO$_3$)) [4] and of adsorbed C_6H_6O "like" molecules on the surface, the reactions involved, in the presence of oxygen, during

Table 2
Percentages deducted from TPO, ATD-ATG and elementary analysis (EA) as well as evolution of the quantity of the carbon-containing deposit according to the addition of %Zr

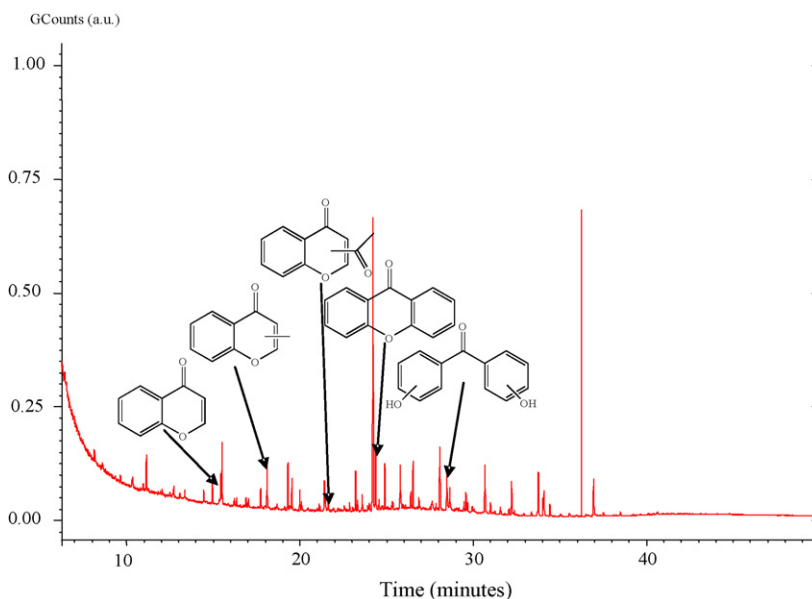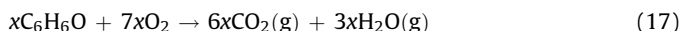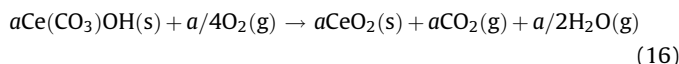| Catalyst	TPO	Elementary analysis		DTA–TGA		mMol g^{-1}			C in CO$_3^{2-}$	C in HC	
	%C	%C	%H	%Loss	%O	n(C)	n(H)	n(O)	a	$6x$	NL
PtCe^c	9.52	9.50	0.51	22.70	12.69	7.93	5.10	7.93	3.61	4.32	0.8
PtCe^{c}650	9.37	9.34	0.48	22.83	13.01	7.80	4.80	8.13	3.73	4.07	0.5
PtCe^{c}800	7.21	8.71	0.46	20.90	13.23	6.63	4.60	8.27	3.91	2.73	0.5
PtCZ(90)	8.70	8.68	0.50	21.70	12.31	7.24	5.00	7.69	3.54	3.70	1.8
PtCZ(75)	6.38	5.90	0.53	11.09	3.66	5.12	5.30	2.29	0.78	4.33	3.5
PtCZ(50)	3.97	3.51	0.36	7.78	3.91	3.12	3.60	2.44	1.05	2.07	10.8
CZ(50)	6.78	6.89	0.68	12.99	6.07	5.70	6.80	3.39	1.33	4.37	0.4

Fig. 6. GC analysis of extracted mixture from PtCe[c] used catalyst. Formula of the identified adsorbed compounds deduced from MS.

the characterization experiments (TPO, TDA–TGA) of used catalysts are:

$$aCe(CO_3)OH(s) + a/4O_2(g) \rightarrow aCeO_2(s) + aCO_2(g) + a/2H_2O(g) \tag{16}$$

$$xC_6H_6O + 7xO_2 \rightarrow 6xCO_2(g) + 3xH_2O(g) \tag{17}$$

From these equations, it is possible to determine the values of a and x where a represents the proportion of carbonate species (C in CO_3^{2-}) and $6x$ the proportion of polymeric carbon species (C in HC):

With, $n(C) = a + 6x$ and $n(O) = x + 2a$

$$a = n(C) - 6X \tag{18}$$

and

$$X = n(O) - 2a = \frac{2n(C) - n(O)}{11} \tag{19}$$

The results of these calculations (Table 2) show higher contents of carbonates (C in CO_3^{2-}) for the catalysts highly loaded in cerium (PtCe and PtCZ(90)). This is mainly due to the strong basicity of these supports. To confirm this, the basicity of the supports was characterized by infrared spectroscopy using the adsorption of CO_2 as a probe molecule. This molecule is adsorbed preferentially on O^{2-} and OH^- sites to form carbonate or hydrogenocarbonate species. According to the environment of oxygen, several types of carbonate species can coexist.

In the 2000–900 cm^{-1} range (Fig. 7), the adsorption of CO_2 leads to the formation of several bands. The bands at 1610, 1403, and 1217 cm^{-1} are due to the hydrogenocarbonate species, whereas, the bands at 1574, 1291 and 1045 cm^{-1} indicate the presence of bidentate carbonate species. Additional bands at 1468 and 1015 cm^{-1} attributed to polydentate species are evidenced [31]. The main result is that an increase of the zirconium content induces a weakening of band intensities and confirms that the basicity of the oxide materials is in inverse proportion with the Zr content. The catalyst carbonatation during phenol WAO (C in CO_3^{2-}) is thus limited for the supports heavily charged in zirconium (PtCZ(75) and PtCZ(50)).

Moreover, concerning the polymeric carbon species (C in HC), the results show a limitation in adsorption of by-products by (i) a

decrease in BET area and/or (ii) for a high loading of Zr (50 wt.%). The comparison between the bare support and the PtCZ(50) catalyst confirms the beneficial effect of platinum addition. On these mixed oxides, the presence of platinum limits the catalyst poisoning by phenol polymerization as well as the carbonatation phenomena.

The insertion of zirconium induces (i) a limitation of the support basicity and thus of the carbonate contents and (ii) for the higher loading of Zr, an easier elimination of polymers by promoting oxygen transfer. This phenomenon is evidenced in the case of PtCZ(50) catalyst presenting the highest NL value.

3.3.3. Correlation between TOF and poisonous species

To determine the intrinsic activity, turn over frequencies (TOF (h^{-1})) were calculated on the basis of the mineralization at 1 h of reaction and then compared to the surface area and polymeric carbon contents in the Table 3.

For the catalysts supported on pure ceria, it appears that the variation of the specific surface area of the support has an influence
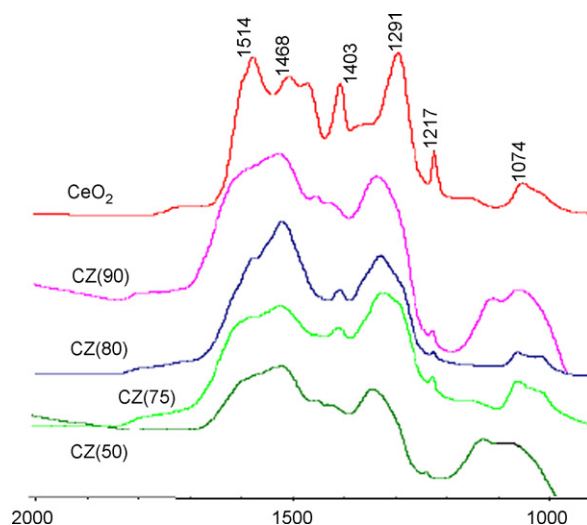

Fig. 7. FT-IR spectra obtained after CO_2 adsorption at ambient temperature on the bare supports activated under air at 450 °C.

Table 3
BET surface area, dispersion, mineralization at 1 h, polymeric carbon specie contents, TOF and surface of contact for all the catalysts

Catalysts	S_{BET} $(m^2\,g^{-1})$	C in HC $(6\times)$ $(mol\,g^{-1})$	$\%M_{1\,h}$ (%)	D (%)	TOF (h^{-1})	$S_{Pt\,contact}/$ S_{BET} (%)
PtCe[c]	184	4.32	23	63	9.4	1.01
PtCe[c]650	96	4.07	27	55	12.8	1.69
PtCe[c]800	45	2.73	32	41	20.4	2.68
PtCZ(90)	59	3.70	31	52	15.6	2.60
PtCZ(75)	84	4.33	16	49	8.5	1.72
PtCZ(50)	50	2.07	36	39	24.1	2.30

on the platinum behavior in reaction since the material presenting the smallest surface area is more active. The classification of the TOF values for the PtCe catalysts is: PtCe[c] < PtCe[c]650 < PtCe[c]800. In term of intrinsic activity, previous works [4] have already showed a similar phenomenon for this type of catalyst since a maximum of activity for acetic acid CWAO has been observed for an optimal metal/support interface corresponding to a 15% of platinum dispersion. In this case, a too high dispersion or a too weak specific surface area induced a poisoning of the catalyst by the carbonate species which inhibited the oxygen transfer. In our case, all the catalysts present similar high dispersions and, for a given support, the smaller the surface the higher the phenol mineralization.

The same phenomenon is observed for the PtCZ catalysts. The TOF value is minimum for the material presenting a zirconium loading of 25 wt.% and for which the BET surface area is the highest. The classification of the TOF values for the PtZC catalysts is: PtCZ(75) < PtCZ(90) < PtCZ(50).

Finally, the intrinsic activities increase for those catalysts having the lowest contents of polymeric carbon species. Moreover, the comparison between the PtCZ(75) and the PtCZ(50) catalysts, which present the same amount in CO_3^{2-}, allows to conclude that the adsorbed species coming from phenol polymerization ("coke") are mainly responsible for catalyst poisoning. In order to explain the different catalyst behavior against deactivation, it seems important to take into account the metal/support interface. Supposing a hemispherical shape of metallic particle, a relative metal/support interface value can be calculated as the ratio between the surface of Pt particles in contact with the support ($S_{Pt\,contact}$ schematized in Fig. 8) and the BET surface area of the considered support.

From the dispersion (D in %), the molar number of platinum per gram of catalyst ($n_{Pt} = 1.28 \times 10^{-4}$ mol g^{-1}) and the surface developed per mole of platinum ($S_{Pt0} = 45293$ m^2 mol^{-1}) [24], the surface of platinum in contact with the support ($S_{Pt\,contact}$) can be calculated by the following equation:

$$S_{Pt\,contact} = \frac{Dn_{Pt}S_{Pt0}}{2 \times 100} \qquad (20)$$

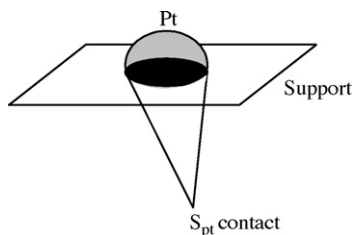where 2 corresponds to the ratio between the surfaces of a hemisphere and a circle.

Fig. 8. Hemispherical model and determination of $S_{Pt\,contact}$.

Relative Pt/support interfaces increase when specific surface areas decrease (Table 3). Both oxygen transfer and "coke" combustion are easier when the relative metal/support interface increases which limits the poisoning. Finally, better is the Pt/support distribution, higher is the phenol mineralization especially on the mixed oxide catalysts Pt(CZ(50)). These results confirm that the oxygen transfer is an essential step in CWAO of phenol.

4. Conclusion

CWAO of aqueous solution of phenol has been carried out with pure oxygen (2 MPa) at 160 °C in a stirred batch reactor on platinum supported oxide catalysts (PtCeO$_2$ and PtCe$_x$Zr$_{1-x}$O$_2$). One of the most limiting factors of the process efficiency is the oxygen transfer at the catalytic surface. Consequently, the objective of this study was to correlate the catalytic activity in CWAO of phenol with the characteristics of the studied materials such as OSC values, BET surface areas and metal dispersions. The OSC measurements performed on the fresh materials show that the introduction of zirconium into the lattice of ceria increases significantly the mobility of oxygen atoms especially in the presence of platinum. The characterizations of the catalysts, performed after reaction, reveal the presence of CCD which induces a poisoning effect of the catalysts. The CCD is divided into two: (i) carbonates and (ii) polymeric carbon species. According to the high basicity of the supports, higher amounts of carbonates are present on pure ceria than on CZ materials. Nevertheless, the poisoning effect of carbonates is not really effective. The main poison phenomenon is due to the formation of polymers as intermediary by-products of phenol oxidation. The adsorption of these species is limited on low specific surface area catalysts and by the introduction of high contents of zirconium into ceria lattice. The highest activities are then observed on PtCe[c]800 and PtCZ(50) materials. Consequently, in order to reach the total conversion of phenol, an exaltation of platinum intrinsic activity can be achieved by improving (i) the Pt/support interface and (ii) the oxygen mobility of the catalysts.

Acknowledgments

References

[1] F.J. Zimmerman, Wet air oxidation of hazardous organics in wastewater. U.S. Patent No. 2,665, 249, 1950.
[2] J. Levec, A. Pintar, Catal. Today 124 (2007) 172–184.
[3] Y.I. Matatov-Meytal, M. Sheintuch, Ind. Eng. Chem. Res. 37 (1998) 309–326.
[4] J. Mikulová, J. Barbier Jr., S. Rossignol, D. Mesnard, C. Kappenstein, D. Duprez, J. Catal. 251 (2007) 172–181.
[5] A. Trovarelli, F. Zamar, J. Llorca, C. De leitenburg, G. Dolcetti, J.T. Kiss, J. Catal. 169 (1997) 490–502.
[6] B.B. Pruden, H. Le, Can. J. Chem. Eng. 54 (1976) 319–325.
[7] A. Santos, P. Yustos, B. Durban, F. Garcia-Ochoa, Ind. Eng. Chem. Res. 40 (2001) 2773–2781.
[8] S.S. Lin, D.J. Chang, C.H. Wang, C.C. Chen, Water Res. 4 (2003) 793–800.
[9] V.S. Mishra, V.V. Mahajani, J.B. Joshi, Ind. Eng. Chem. Res. 34 (1995) 2–48.
[10] A. Pichard, M. Bisson, R. Diderich, G. Lacroix, J.P. Lefevre, S. Leveque, H. Magaud, C. Villey, INERIS – Fiche de données toxicologiques et environnementales des substances chimiques: Phénol; http://www.ineris.fr.
[11] H.R. Devlin, I.J. Harris, Ind. Eng. Chem. Res. Fundam. 23 (1984) 387–397.
[12] J. Barbier Jr., F. Delanoë, F. Jabouille, D. Duprez, G. Blanchard, P. Isnard, J. Catal. 177 (1998) 378–385.
[13] L. Li, P. Chen, E.F. Gloyna, AIchE J. 37 (1991) 1687–1697.
[14] S. Hamoudi, F. Larachi, A. Sayari, J. Catal. 177 (1998) 247–258.
[15] F. Stüber, J. Font, A. Fortuny, C. Bengoa, A. Eftaxias, A. Fabregat, Top. Catal. 33 (2005) 3–50.
[16] I.P. Chen, S.S. Lin, C.H. Wang, S.H. Chang, Chemosphere 66 (2007) 172–178.
[17] J. Barbier Jr., L. Oliviero, B. Renard, D. Duprez, Top. Catal. 33 (2005) 77–86.

[18] P. Massa, F. Ivorra, P. Haure, F. Medina Cabello, R. Fenoglio, Catal. Commun. 8 (2007) 424–428.
[19] A. Cybulski, J. Trawkziński, Appl. Catal. B: Env. 47 (2004) 1–13.
[20] Z.P.G. Masende, B.F.M. Kuster, K.J. Ptasinski, F.J.J.G. Janssen, J.H.Y. Katima, J.C. Schouten, Catal. Today 79-80 (2003) 357–370.
[21] D. Duprez, J. Phys. Chem. 80 (1983) 487–505.
[22] V. Perrichon, L. Retailleau, P. Bazin, M. Daturi, J.C. Lavalley, Appl. Catal. 260 (2004) 1–8.
[23] T.R. Hughes, R.H. Houston, R.P. Sieg, 135th Natl. Meeting Am. Chem. Soc. Div. Petrol., Cmem., Prepints, 4, (1959), C33.
[24] J.R. Anderson, Structure of Metallic Catalysts, Academic Press, 1975,, p. 296.
[25] J. Mikulová, S. Rossignol, F. Gérard, D. Mesnard, C. Kappenstein, D. Duprez, J. Solid States Chem. 179 (2006) 2496–2505.
[26] S. Bedrane, C. Descorme, D. Duprez, Catal. Today 75 (2002) 401–405.
[27] M. Guisnet, P. Magnoux, Appl. Catal. 54 (1989) 1–27.
[28] J. Mikulová, S. Rossignol, J. Barbier Jr., D. Mesnard, C. Kappenstein, D. Duprez, Appl. Catal. B: Env. 72 (2007) 1–10.
[29] L. Oliviero, Thesis of University of Poitiers, (2001).
[30] D. Duprez, F. Delanoë, J. Barbier Jr., P. Isnard, G. Blanchard, Catal. Today 29 (1996) 317–322.
[31] C. Binet, A. Jadi, J.C. Lavalley, J. Chim. Phys. 89 (1992) 31–45.